

Supplementary material for manuscript:

Reactivity of the free and (5,5)-carbon nanotube supported AuPt bimetallic clusters towards O₂ activation. A theoretical study

Fazel Shojaei¹, Masoumeh Mousavi¹, Fariba Nazari^{1,2}, Francesc Illas³

¹*Department of Chemistry, Institute for Advanced Studies in Basic Sciences, Zanjan 45137-66731, Iran*

²*Center of Climate Change and Global Warming, Institute for Advanced Studies in Basic Sciences, Zanjan 45137-66731, Iran*

³*Departament de Química Física & Institut de Química Teòrica i Computacional (IQTCUB), Universitat de Barcelona, C/Martí i Franquès 1, 08028 Barcelona, Spain*

The most stable structures and most salient features of the Au_mPt_n ($2 \leq m+n \leq 5$) clusters are presented in Fig. S1. Additional information regarding higher energy isomers and relative stability are provided in Fig. S2 to S4. The binding energy per atom increases with the cluster size and alloying Pt clusters with Au is energetically unfavorable as recently discussed.¹ The tendency of the systems to form clusters with the largest possible number of platinum atoms is clear from the plots in Fig. S4. The HOMO-LUMO gaps reported in Fig. S5 give evidence that pure Au_m clusters exhibit the even-odd oscillation behavior with $E_{\text{H-L}}(\text{even}) > E_{\text{H-L}}(\text{odd})$, which is consistent with other previous reports for this group of clusters.²⁻⁶ Figures S6 and S7 present the electron density distribution of relevant orbitals. Finally, Figures S8 ,S9 and S10 displays the total density of states and its projection on s and d orbitals of Au and Pt atoms in a selected series of clusters. Overall, a general feature emerges among all the studied Au/Pt bimetallic clusters, regardless of their composition; namely, the Pt (5d) states constitute the major contribution to the DOS near the Fermi level and the Au (5d) states appear quite below. The presence of the Pt (5d) states close to the Fermi level implies a larger potential chemical activity of Pt sites in electrophilic and nucleophilic reactions.

Figure S1. The lowest energy structures of pure Au_m , Pt_n ($m, n=2-5$) and binary Au_mPt_n ($2 \leq m+n \leq 5$) alloys, their corresponding bonding energies, E_b (eV/atom), HOMO-LUMO energy gap, $E_{\text{H-L}}$ (eV) and spin magnetic moment, μ (μ/cell).

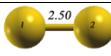
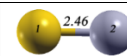
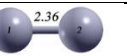
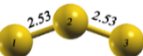
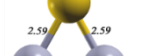
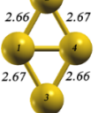
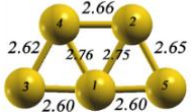
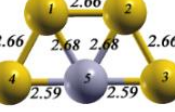
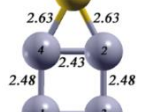
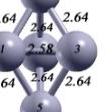
| Au_2 | AuPt | Pt_2 | | | |
|--|--|--|---|--|--|
|  $E_b=-1.17$ $E_{\text{H-L}}=1.96$ $\mu=0$ |  $E_b=-1.27$ $E_{\text{H-L}}=0.09$ $\mu=1$ |  $E_b=-1.75$ $E_{\text{H-L}}=0.27$ $\mu=2$ | | | |
| Au_3 | Au_2Pt | AuPt_2 | Pt_3 | | |
|  $E_b=-1.24$ $E_{\text{H-L}}=0.48$ $\mu=1$ |  $E_b=-1.61$ $E_{\text{H-L}}=0.54$ $\mu=0$ |  $E_b=-1.91$ $E_{\text{H-L}}=0.15$ $\mu=1$ |  $E_b=-2.34$ $E_{\text{H-L}}=0.19$ $\mu=2$ | | |
| Au_4 | Au_3Pt | Au_2Pt_2 | AuPt_3 | Pt_4 | |
|  $E_b=-1.55$ $E_{\text{H-L}}=1.00$ $\mu=0$ |  $E_b=-1.76$ $E_{\text{H-L}}=0.44$ $\mu=1$ |  $E_b=-2.03$ $E_{\text{H-L}}=0.20$ $\mu=2$ |  $E_b=-2.32$ $E_{\text{H-L}}=0.08$ $\mu=3$ |  $E_b=-2.64$ $E_{\text{H-L}}=0.20$ $\mu=4$ | |
| Au_5 | Au_4Pt | Au_3Pt_2 | Au_2Pt_3 | AuPt_4 | Pt_5 |
|  $E_b=-1.62$ $E_{\text{H-L}}=0.44$ $\mu=1$ |  $E_b=-1.93$ $E_{\text{H-L}}=0.37$ $\mu=0$ |  $E_b=-2.13$ $E_{\text{H-L}}=0.33$ $\mu=1$ |  $E_b=-2.38$ $E_{\text{H-L}}=0.16$ $\mu=2$ |  $E_b=-2.64$ $E_{\text{H-L}}=0.24$ $\mu=1$ |  $E_b=-2.88$ $E_{\text{H-L}}=0.44$ $\mu=4$ |

Figure S2. Au_nPt_m ($m+n \leq 5$) structural isomers E_b (eV/atom) is the representative of the energy

difference between structural isomers and ground state and μ (μ/cell). is the magnetic moment.

| | Au_3^1 | Au_2Pt^1 | Au_2Pt^2 | AuPt_2^1 | AuPt_2^2 | Pt_3^1 |
|------------|----------------------------|----------------------------|----------------------------|--------------------------|----------------------------|----------------------------|
| ΔE | 0.0459 | 0.115 | 0.236 | 0.05 | 0.331 | 0.186 |
| μ_B | 1 | 2 | 2 | 3 | 3 | 4 |
| | Au_4^1 | Au_4^2 | Au_3Pt^1 | Au_3Pt^2 | Au_2Pt_2^1 | Au_2Pt_2^2 |
| ΔE | 0.001 | 0.170 | 0.019 | 0.063 | 0.001 | 0.012 |
| μ_B | 0 | 2 | 1 | 1 | 2 | 2 |
| | Au_2Pt_2^3 | Au_2Pt_2^4 | Au_2Pt_2^5 | AuPt_3^1 | AuPt_3^2 | AuPt_3^3 |
| ΔE | 0.069 | 0.078 | 0.148 | 0.007 | 0.021 | 0.040 |
| μ_B | 0 | 2 | 2 | 1 | 1 | 3 |
| | Pt_4^1 | Pt_4^2 | Pt_4^3 | Au_5^1 | Au_5^2 | Au_5^3 |
| ΔE | 0.003 | 0.01 | 0.042 | 0.081 | 0.114 | 0.135 |
| μ_B | 2 | 4 | 6 | 1 | 1 | 1 |
| | Au_5^4 | Au_5^5 | Au_5^6 | Au_4Pt^1 | Au_4Pt^2 | Au_4Pt^3 |
| ΔE | 0.196 | 0.200 | 0.206 | 0.080 | 0.080 | 0.128 |
| μ_B | 1 | 1 | 1 | 0 | 2 | 0 |

Figure S2 continued

| | | | | | | |
|------------|-------|-------|-------|-------|-------|-------|
| ΔE | 0.130 | 0.145 | 0.017 | 0.026 | 0.033 | 0.052 |
| μ_B | 0 | 2 | 1 | 1 | 3 | 3 |
| ΔE | 0.056 | 0.063 | 0.078 | 0.030 | 0.031 | 0.061 |
| μ_B | 1 | 1 | 1 | 2 | 2 | 4 |
| ΔE | 0.066 | 0.077 | 0.089 | 0.100 | 0.005 | 0.014 |
| μ_B | 2 | 2 | 2 | 2 | 3 | 3 |
| ΔE | 0.035 | 0.047 | 0.060 | 0.154 | 0.017 | 0.020 |
| μ_B | 3 | 1 | 5 | 1 | 6 | 2 |
| ΔE | 0.021 | 0.047 | 0.052 | 0.091 | | |
| μ_B | 4 | 4 | 4 | 2 | | |

Figure S3. Binding energy of Au_mPt_n ($m+n \leq 5$) bimetallic cluster as the function of cluster composition (m/n). Different colors serve as an eye guide only.

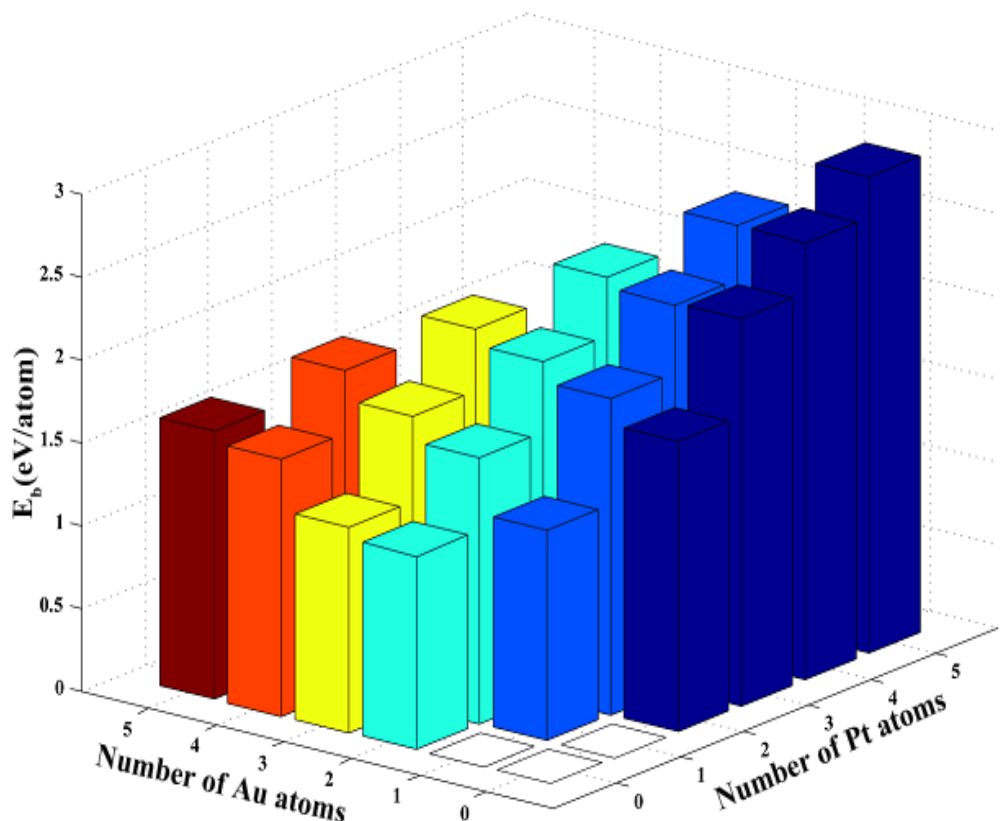


Figure S4. Atom attachment energy, E_{int} (eV/atom) , for Au_mPt_n bimetallic clusters. Green color represents the attachment energy of Au atom to Au_mPt_n bimetallic clusters and, and blue color represents the attachment energy of Pt atom to Au_mPt_n bimetallic clusters. Different colors serve as an eye guide only.

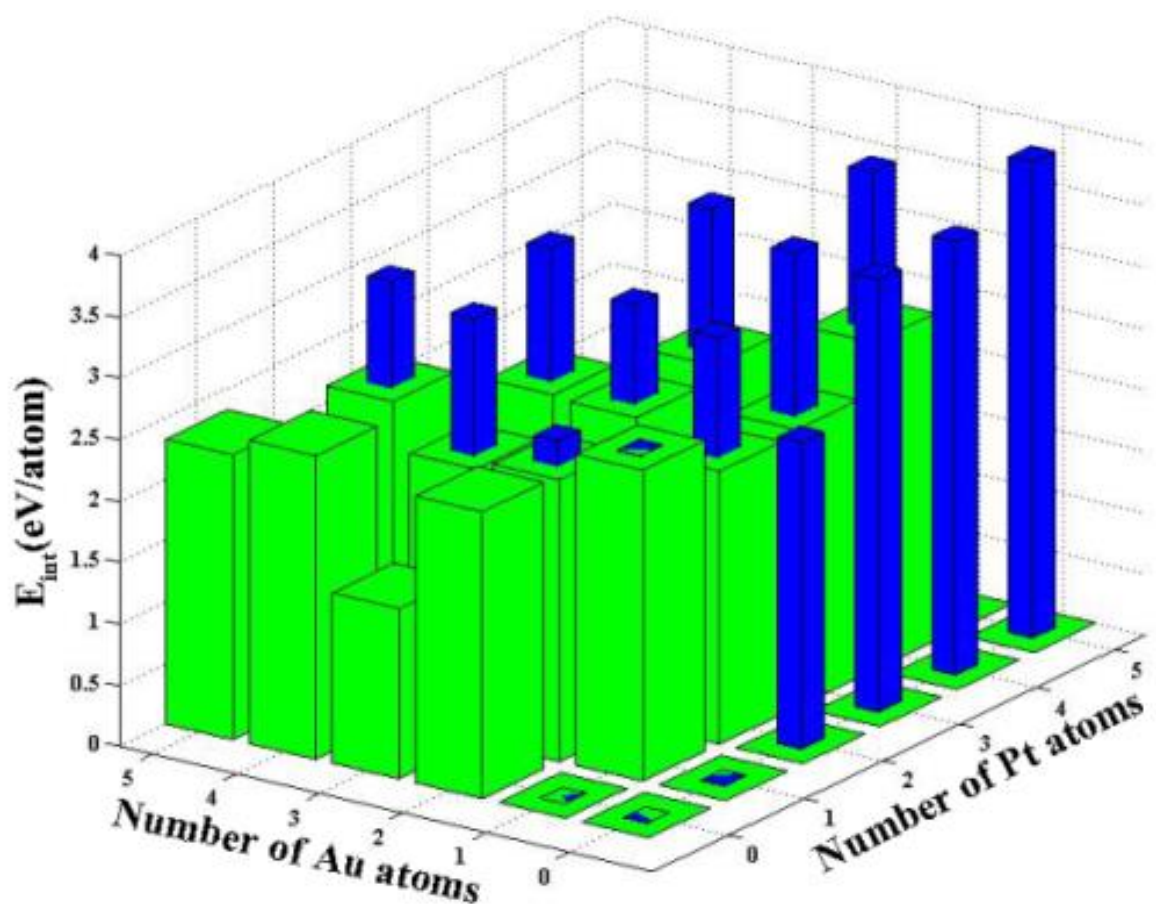


Figure S5. HOMO-LUMO energy gap, E_{H-L} , of Au_mPt_n ($m+n\leq 5$) bimetallic clusters as the function of cluster composition. Different colors serve as an eye guide only.

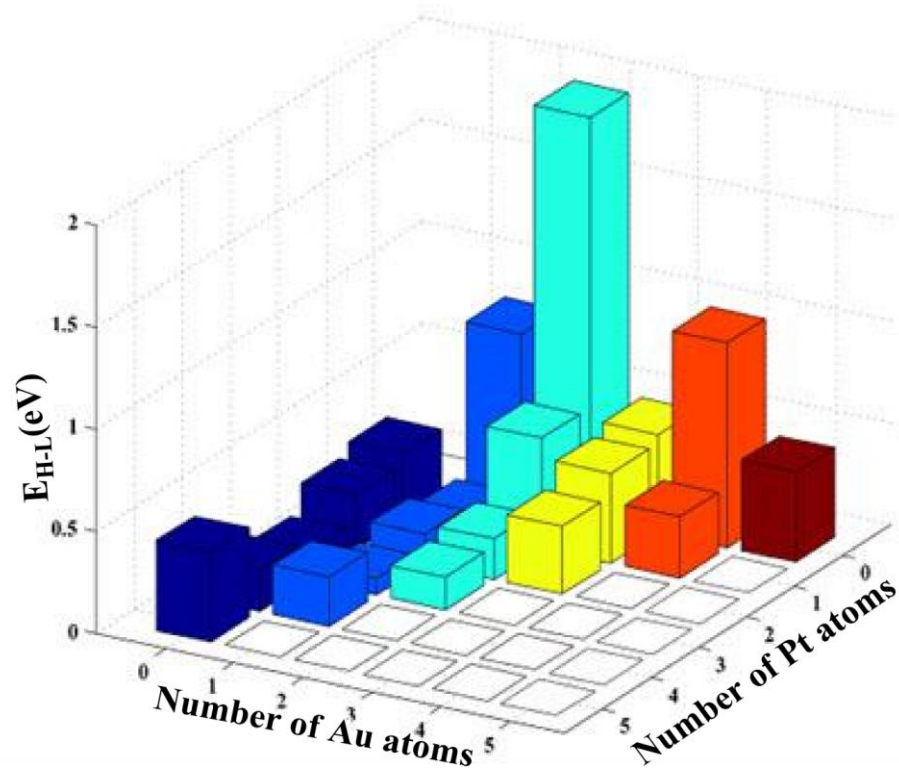


Figure S6. HOMO and LUMO electron density of some representative mono- and bimetallic clusters.

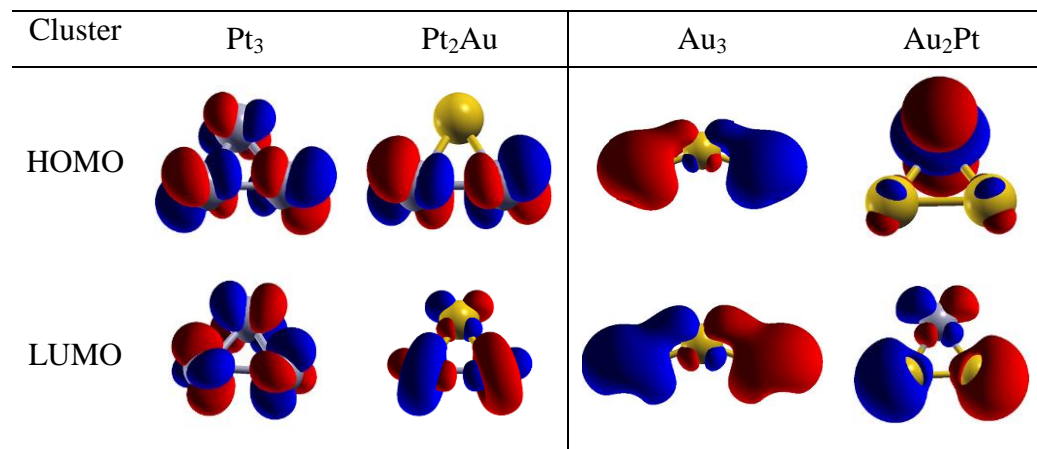


Figure S7. HOMO and LUMO electron density of Au_nPt_m ($m+n \leq 5$) metallic and bimetallic clusters.

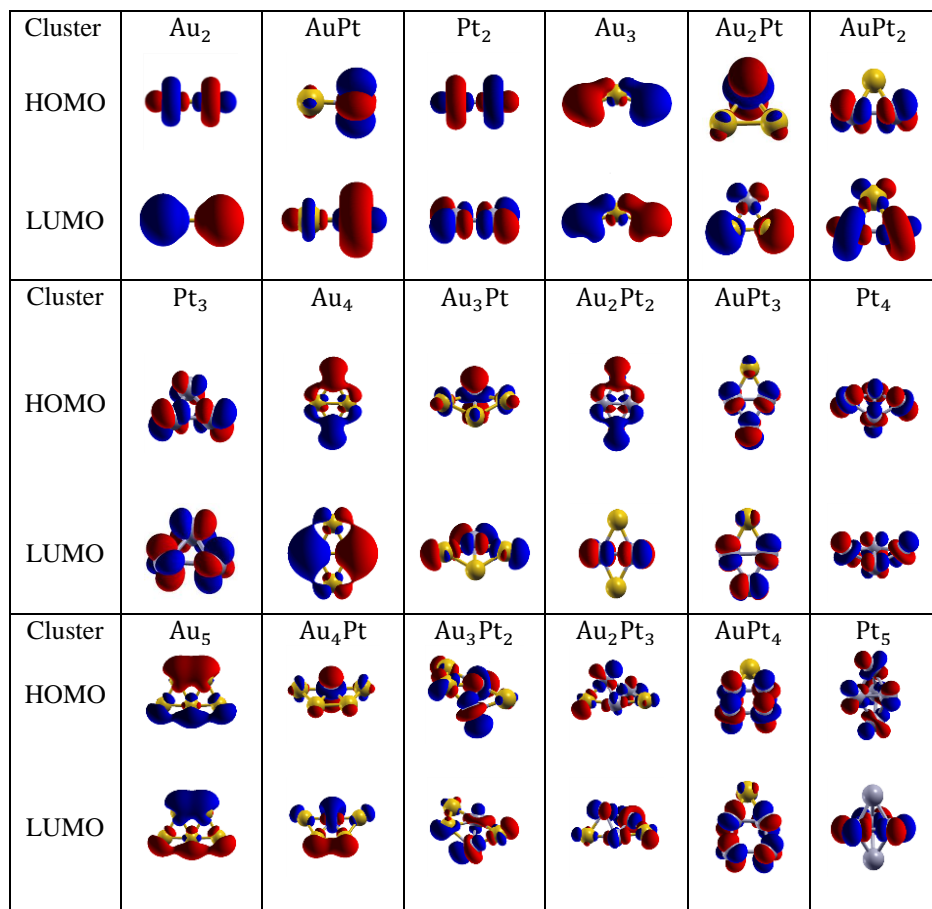


Figure S8. Plots of density of states projected on s and d orbitals of Pt and Au in their corresponding clusters.

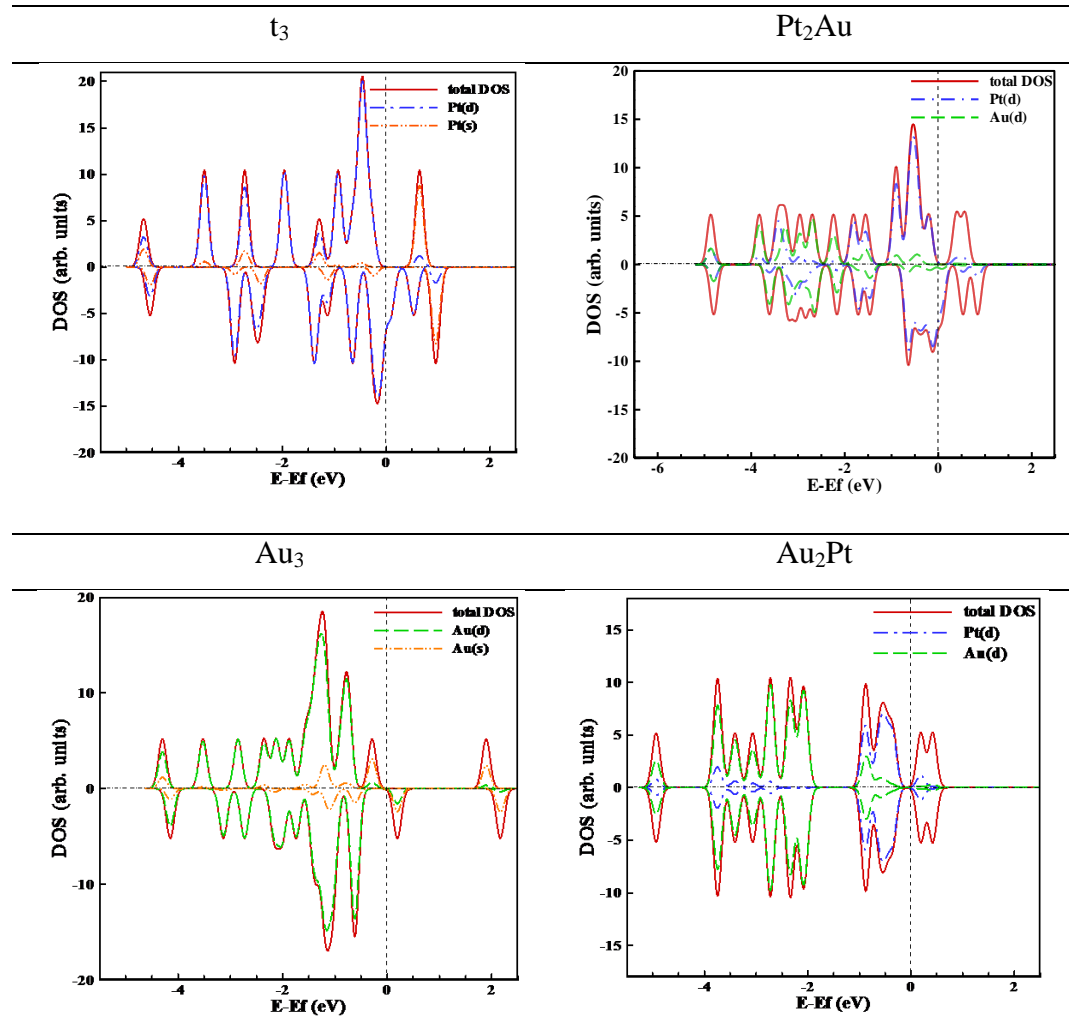


Figure S9. s and d orbital density of states and projected density of states of Au_nPt_m ($m+n \leq 4$) metallic and bimetallic clusters.

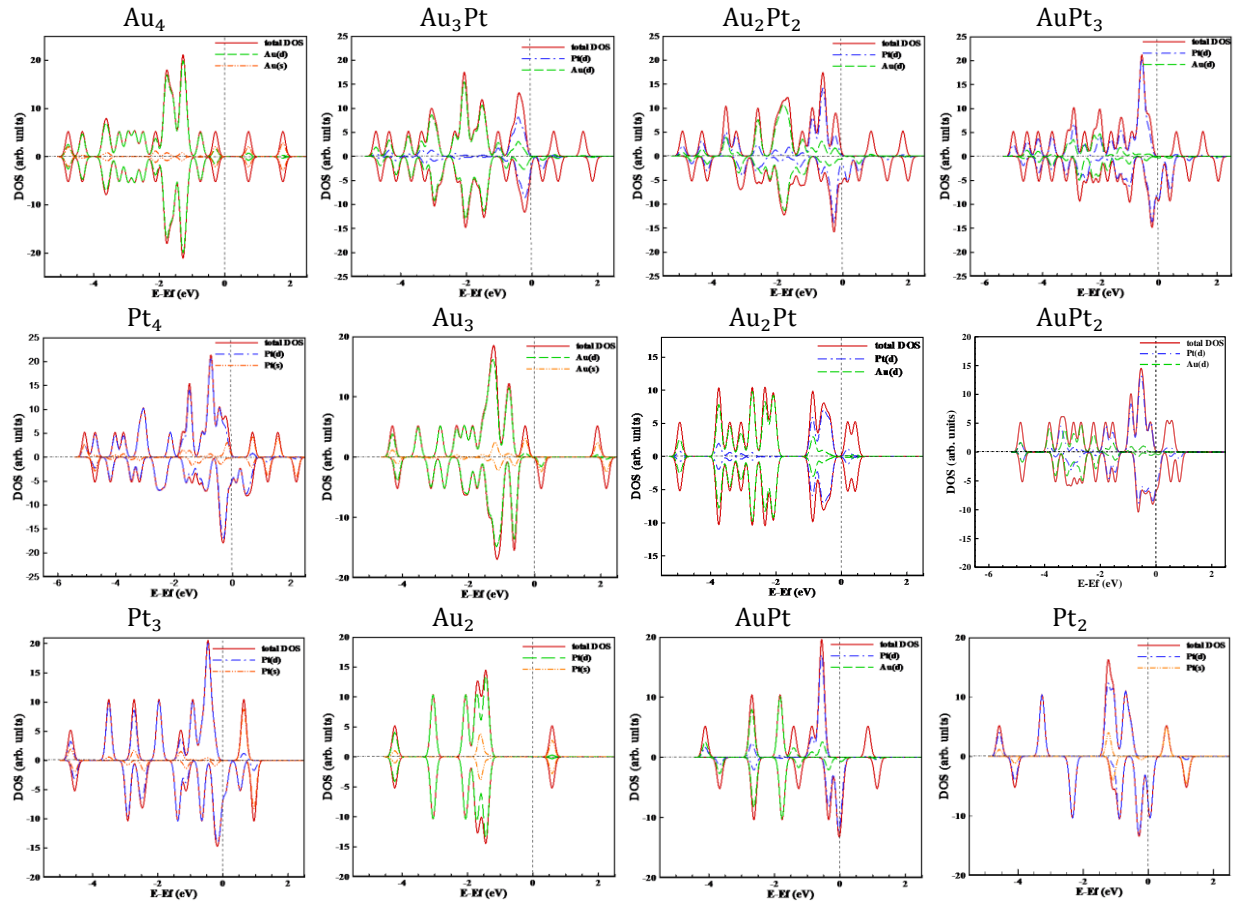


Figure S10. s and d orbital density of states and projected density of states of Au_nPt_m ($m+n=5$) metallic and bimetallic clusters.

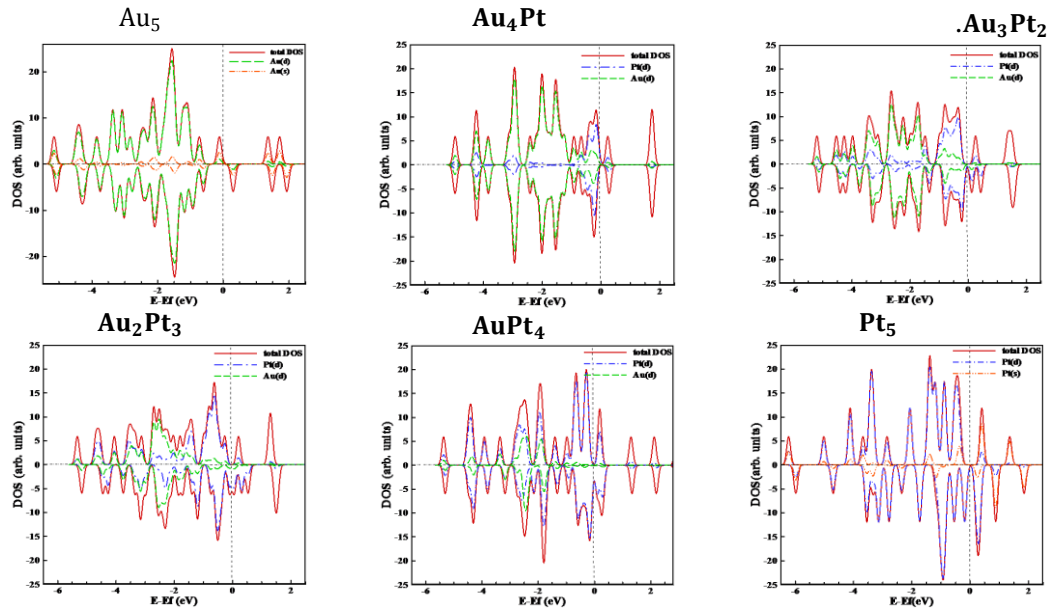


Figure S11. $\text{Au}_n\text{Pt}_m\text{O}_2$ ($m+n \leq 5$) stable structures and spin magnetic moment μ (μ/cell)

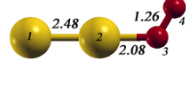
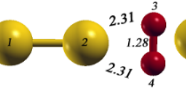
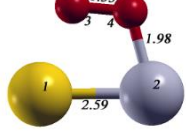
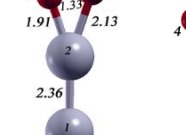
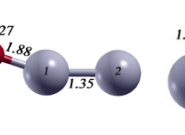
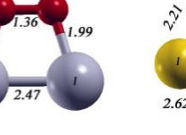
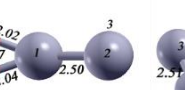
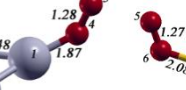
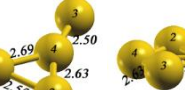
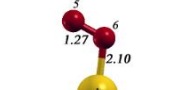
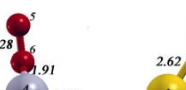
| | $\text{Au}_2\text{O}_2^{\text{g}}$ | $\text{Au}_2\text{O}_2^{\text{l}}$ | $\text{AuPtO}_2^{\text{g}}$ | $\text{AuPtO}_2^{\text{l}}$ | $\text{AuPtO}_2^{\text{2}}$ | $\text{AuPtO}_2^{\text{3}}$ |
|---|---|---|--|---|---|---|
|  | |  |  |  |  |  |
| E_b | 0.51 | 0.27 | 1.54 | 1.53 | 1.33 | 0.52 |
| μ_B | 2 | 2 | 1 | 1 | 1 | 3 |
| | $\text{AuPtO}_2^{\text{4}}$ | $\text{Pt}_2\text{O}_2^{\text{g}}$ | $\text{Pt}_2\text{O}_2^{\text{l}}$ | $\text{Pt}_2\text{O}_2^{\text{2}}$ | $\text{Au}_3\text{O}_2^{\text{g}}$ | $\text{Au}_2\text{PtO}_2^{\text{g}}$ |
|  |  |  |  |  |  | |
| E_b | 0.40 | 1.31 | 1.21 | 1.09 | 0.75 | 1.53 |
| μ_B | 3 | 2 | 0 | 1 | 1 | 2 |
| | $\text{Au}_2\text{PtO}_2^{\text{1}}$ | $\text{Au}_2\text{PtO}_2^{\text{2}}$ | $\text{AuPt}_2\text{O}_2^{\text{g}}$ | $\text{AuPt}_2\text{O}_2^{\text{l}}$ | $\text{AuPt}_2\text{O}_2^{\text{2}}$ | $\text{AuPt}_2\text{O}_2^{\text{3}}$ |
|  |  |  |  |  |  | |
| E_b | 1.30 | 0.68 | 2.08 | 1.77 | 1.30 | 0.77 |
| μ_B | 2 | 2 | 1 | 1 | 1 | 3 |
| | $\text{Pt}_3\text{O}_2^{\text{g}}$ | $\text{Pt}_3\text{O}_2^{\text{l}}$ | $\text{Pt}_3\text{O}_2^{\text{2}}$ | $\text{Pt}_3\text{O}_2^{\text{3}}$ | $\text{Au}_4\text{O}_2^{\text{g}}$ | $\text{Au}_4\text{O}_2^{\text{l}}$ |
|  |  |  |  |  |  | |
| E_b | 1.58 | 1.56 | 1.39 | 1.30 | 0.54 | 0.53 |
| μ_B | 2 | 0 | 2 | 0 | 2 | 2 |
| | $\text{Au}_4\text{O}_2^{\text{2}}$ | $\text{Au}_4\text{O}_2^{\text{3}}$ | $\text{Au}_3\text{PtO}_2^{\text{g}}$ | $\text{Au}_3\text{PtO}_2^{\text{l}}$ | $\text{Au}_3\text{PtO}_2^{\text{2}}$ | $\text{Au}_3\text{PtO}_2^{\text{3}}$ |
|  |  |  |  |  |  | |
| E_b | 0.50 | 0.17 | 1.69 | 1.33 | 1.02 | 0.64 |
| μ_B | 2 | 0 | 1 | 1 | 3 | 3 |

Figure S11 Continued

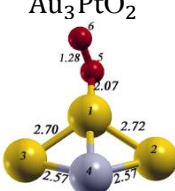
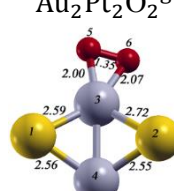
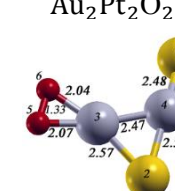
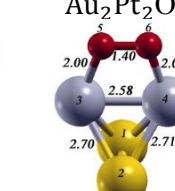
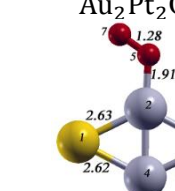
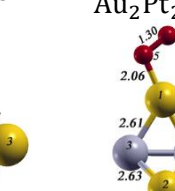
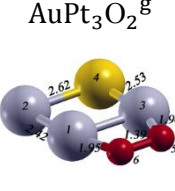
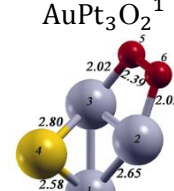
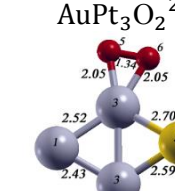
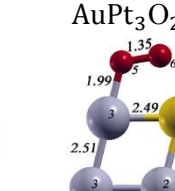
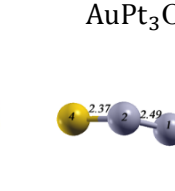
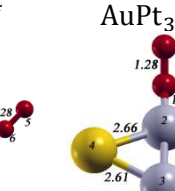
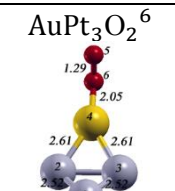
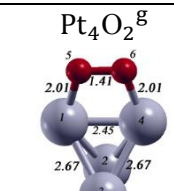
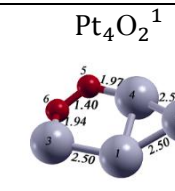
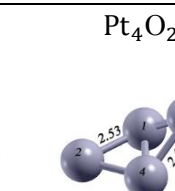
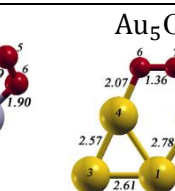
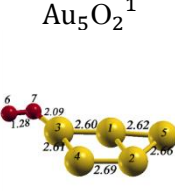
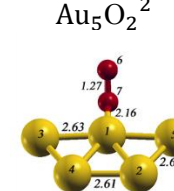
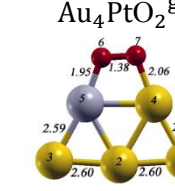
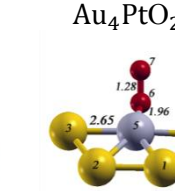
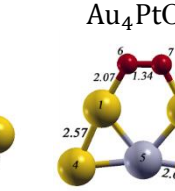
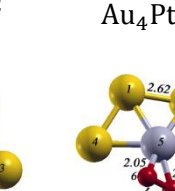
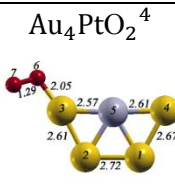
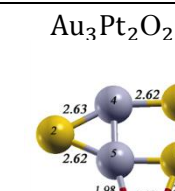
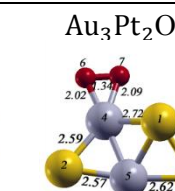
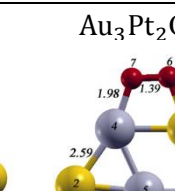
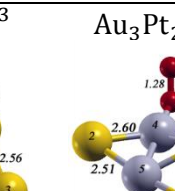
| | | | | | | |
|---|---|---|---|---|---|-----------|
| $\text{Au}_3\text{PtO}_2^4$ | $\text{Au}_2\text{Pt}_2\text{O}_2^g$ | $\text{Au}_2\text{Pt}_2\text{O}_2^1$ | $\text{Au}_2\text{Pt}_2\text{O}_2^2$ | $\text{Au}_2\text{Pt}_2\text{O}_2^3$ | $\text{Au}_2\text{Pt}_2\text{O}_2^4$ | |
|  |  |  |  |  |  | |
| E_b μ_B | 0.40 1 | 1.55 2 | 1.50 0 | 1.30 2 | 1.15 2 | 0.65 2 |
| $\text{AuPt}_3\text{O}_2^g$ | $\text{AuPt}_3\text{O}_2^1$ | $\text{AuPt}_3\text{O}_2^2$ | $\text{AuPt}_3\text{O}_2^3$ | $\text{AuPt}_3\text{O}_2^4$ | $\text{AuPt}_3\text{O}_2^5$ | |
|  |  |  |  |  |  | |
| E_b μ_B | 1.97 1 | 1.59 1 | 1.51 3 | 1.39 1 | 1.36 1 | 1.26 1 |
| $\text{AuPt}_3\text{O}_2^6$ | Pt_4O_2^g | Pt_4O_2^1 | Pt_4O_2^2 | Pt_4O_2^3 | Au_5O_2^g | |
|  |  |  |  |  |  | |
| E_b μ_B | 0.73 1 | 1.64 2 | 1.43 2 | 1.40 4 | 1.22 2 | 1.18 1 |
| Au_5O_2^1 | Au_5O_2^2 | $\text{Au}_4\text{PtO}_2^g$ | $\text{Au}_4\text{PtO}_2^1$ | $\text{Au}_4\text{PtO}_2^2$ | $\text{Au}_4\text{PtO}_2^3$ | |
|  |  |  |  |  |  | |
| E_b μ_B | 0.56 1 | 0.38 1 | 1.57 2 | 0.91 0 | 0.83 2 | 0.63 0 |
| $\text{Au}_4\text{PtO}_2^4$ | $\text{Au}_3\text{Pt}_2\text{O}_2^g$ | $\text{Au}_3\text{Pt}_2\text{O}_2^1$ | $\text{Au}_3\text{Pt}_2\text{O}_2^2$ | $\text{Au}_3\text{Pt}_2\text{O}_2^3$ | $\text{Au}_3\text{Pt}_2\text{O}_2^4$ | |
|  |  |  |  |  |  | |
| E_b | 0.39 | 2.50 | 1.71 | 1.55 | 1.49 | 1.25 |
| μ_B | 0 | 1 | 1 | 1 | 3 | 1 |

Figure S11 continued

Figure S12. Top and side view of the (5,5)-CNT supported metal-O₂ complexes along with adsorption energy and spin magnetic moment μ (μ/cell)

| O ₂ Au@CNT | O ₂ Pt@CNT | O ₂ Au ₂ @CNT | O ₂ AuPt@CNT | O ₂ Pt ₂ @CNT |
|---------------------------------------|---|---------------------------------------|---------------------------------------|---------------------------------------|
| | | | | |
| ΔE 0.66 μ_B 0 | ΔE 1.42 μ_B 0.01 | ΔE 0.13 μ_B 1.98 | ΔE 0.15 μ_B 1.31 | ΔE 2.01 μ_B 0.05 |
| O ₂ Au ₃ @CNT | O ₂ Au ₂ Pt@CNT | O ₂ AuPt ₂ @CNT | O ₂ Pt ₃ @CNT | O ₂ Au ₄ @CNT |
| | | | | |
| ΔE 0.90 μ_B 1.11 | ΔE 0.70 μ_B 1.20 | ΔE 0.33 μ_B 1.41 | ΔE 1.06 μ_B 0 | ΔE 0.97 μ_B 0.56 |
| O ₂ Au ₃ Pt@CNT | O ₂ Au ₂ Pt ₂ @CNT | O ₂ AuPt ₃ @CNT | O ₂ Pt ₄ @CNT | |
| | | | | |
| ΔE 0.46 μ_B 1.21 | ΔE 1.37 μ_B 0 | ΔE 1.82 μ_B 0 | ΔE 1.09 μ_B 0.01 | |

-
- ¹ H. K. Yuan, A. L. Kuang, C. L. Tian, and H. Chen, *AIP Adv.*, 2014, **4**, 037107.
 - ² L. Xiao and L. Wang, *J. Phys. Chem. A*, 2004, **108**, 8605.
 - ³ K. Bhattacharyya and C. Majumder, *Chem. Phys. Lett.*, 2007, **446**, 374.
 - ⁴ F. Wang, P. Liu and D. Zhang, *J. Mol. Model.*, 2011, **17**, 1069.
 - ⁵ H. Hakkinen and U. Landman, *Phys. Rev. B: Condens. Matter*, 2000, **62**, R2287.
 - ⁶ W. Hong-Yan, L. Xi-Bo, T. Yong-Jian, R. B. King and H. F. Schaefer III., *Chin. Phys.*, 2007, **16**, 1660.